New Algorithm for Selecting Meniscal Allografts that Best Match the Size and Shape of the Damaged Meniscus

Tommy L. Haut Donahue,[1] Maury L. Hull,[2,3] Stephen M. Howell[2]

[1]Department of Mechanical Engineering, Michigan Technological University, Houghton, Michigan 49931

[2]Department of Mechanical Engineering, University of California, Davis, California 95616

[3]Biomedical Engineering Program, University of California, Davis, California 95616

Received 15 February 2005; accepted 8 June 2005

Published online 26 May 2006 in Wiley InterScience (www.interscience.wiley.com). DOI 10.1002/jor.20155

ABSTRACT: Procedures used by tissue banks in selecting meniscal allografts that will best restore normal contact pressure at the time of surgical implantation into a recipient's knee should be improved. Our objective was to develop regression equations that use dimensions measured from magnetic resonance (MR) images of the contralateral knee to predict values of important meniscal parameters of the injured knee. Another objective was to incorporate these equations into an algorithm for selecting allografts that best match the size and shape of the damaged meniscus (either medial or lateral). In each of 10 knee specimens, four transverse and six cross-sectional parameters of the medial and lateral menisci were quantified from measurements obtained using a laser-based, noncontacting, 3-D coordinate digitizing system. In each of 10 contralateral knee specimens, six transverse and 24 cross-sectional (i.e., perpendicular to transverse plane) dimensions were measured for the medial and lateral menisci from MR images of each knee specimen. Simple linear regression equations related these 10 parameters to each of 38 predictor variables determined from magnetic resonance imaging (MRI) dimensions and the best regression equation for each parameter was identified. Requiring only 9 of the 30 dimensions as predictor variables, the best regression equations predicted 8 of 10 and 10 of 10 medial and lateral menisci parameters, respectively, with R^2 values >0.500. The algorithm for selecting meniscal allografts involves: collecting an inventory of meniscal allografts and determining the 10 meniscus parameter values for all allografts in the inventory; measuring the dimensions as required from MRI scans of the uninjured knee; using the dimensions as inputs to the regression equations to predict values of meniscal parameters; and selecting the meniscal allograft from the inventory that best matches the predicted values of meniscal parameters. Selecting meniscal allografts using our new algorithm may enable allografts to better meet the clinical objectives of meniscal transplantation, which are to reduce pain in some patients following meniscal resection and to inhibit the degeneration of the articular cartilage.
© 2006 Orthopaedic Research Society. Published by Wiley Periodicals, Inc. J Orthop Res 24:1535–1543, 2006

Keywords: meniscus; size; MRI; knee; tissue bank; allograft; replacement; donor; recipient

INTRODUCTION

The two primary goals of meniscal transplantation are to reduce pain experienced by some patients following meniscectomy and to prevent degenerative changes of cartilage following meniscectomy.[1] Both pain and degenerative changes occur in the articular cartilage presumably because of decreased contact area and corresponding increased contact pressure that develops between the cartilage surfaces when the meniscus is resected.[2–4] Because the contact pressure increases in direct proportion to the amount of meniscus removed,[3] the whole of the tissue is required in the joint to prevent increased contact pressure and hence reduce the pain and retard degenerative changes following meniscectomy. One treatment option that satisfies this requirement is meniscal transplantation.

For meniscal transplants or allografts to be successful clinically, they must meet both biological and biomechanical criteria. Among the biological criteria are: transplantation without an adverse immunological response; repopulation by cells which restore normal biosynthetic activities; and healing to the surrounding tissues with revascularization. One important biomechanical criterion

Correspondence to: Maury L. Hull, Department of Mechanical Engineering, University of California, Davis, CA 95616. (Telephone: 530-752-6220; Fax: 530-752-4158; E-mail: mlhull@ucdavis.edu)

© 2006 Orthopaedic Research Society. Published by Wiley Periodicals, Inc.

WILEY InterScience® DISCOVER SOMETHING GREAT

is that the contact pressure distribution on the tibial plateau be restored closely to normal.

Although the biological criteria appear to be largely satisfied in humans,[5] the biomechanical criterion is not consistently satisfied using current procedures to select meniscal allografts.[4,6] Accordingly, developing procedures to select meniscal allografts so that they more consistently restore contact pressure to normal at the time of implantation may enable allografts to either prevent or decelerate degenerative arthritis. Also allografts that restore contact pressure closely to normal may be less susceptible to failure, which has been observed clinically.[7–9]

One factor that must be considered in selecting meniscal allografts is geometric similarity.[10] Both transverse and cross-sectional (i.e., perpendicular to transverse plane) geometric features are important determinants of the contact pressure.[11,12] However, existing procedures used to select meniscal allografts attempt to match only transverse geometric parameters, not cross-sectional parameters.[13] Thus, our goal was to develop a new algorithm for selecting meniscal allografts that considers both transverse and cross-sectional parameters. Because magnetic resonance imaging (MRI) has been shown to be a better tool than roentgenography for predicting both transverse parameters[14,15] and cross-sectional parameters[14,15] of menisci, any new algorithm should rely on dimensions measured from magnetic resonance (MR) images rather than from roentgenograms.

To fulfill our goal, we had three specific objectives. The first was to develop regression equations for determining values of important transverse and cross-sectional parameters from dimensions measured in MR images. A related second objective was to evaluate the potential effectiveness in using these equations to select meniscal allografts by determining the differences between predicted parameter values and actual parameter values. For the regression equations to be useful clinically, they must be incorporated into an algorithm that could be used by a technician working in a tissue bank to select a meniscal allograft that best matches the size and shape of the damaged meniscus. Thus, the third objective was to demonstrate how these regression equations could be incorporated into such an algorithm.

METHODS

To develop the regression equations needed to satisfy the first objective, values of dimensions measured from MR images and values of parameters describing the size and shape of the menisci from a previous study were used.[14] Procedural aspects used to acquire these data that are essential to understanding the present article are included in the description below.

Both roentgenography and MRI were used to evaluate 10 pairs of cadaveric knees prospectively and to assure they were free from degenerative arthritis, chondrocalcinosis, and meniscal tears. The pairs were from four males and six females (average age 65 years, range 37–78 years). These same MR images were subsequently used for making bony and meniscal measurements. Because the recipient's contralateral knee (which had an intact meniscus) was used to determine dimensions from which an allograft would be selected, measurements were made on MR images from a randomly selected knee (either right or left) of a pair. Imaging was performed using a 1.5 Tesla scanner (Signa, General Electric Co., Milwaukee, WI) with a dedicated knee coil. Further details including the imaging parameters are available.[14]

The other knee of the pair was disarticulated, and a laser-based noncontacting 3-D coordinate digitizing system (3-DCDS) was used to acquire the 3-D geometry of the medial and lateral menisci with an accuracy of 15 μm.[16] Briefly, a computer representation of each meniscus was created by measuring the surface contours of the menisci and tibial plateau, and then subtracting the surface contour of the tibial plateau measured with the menisci excised. Using the computer representation, a standardized transverse plane was determined for each tibia by performing a least squares regression on the data points of the tibial plateau scanned without the menisci. Anterior was defined by a line drawn perpendicular to a line joining the posterior osteochondral junction of the medial and lateral compartments.

Four standard transverse parameters for each meniscus were described by measuring four distances in the standardized transverse plane (Fig. 1a): the depth (AP depth), the ratio of enclosure (ratio), the maximum width of the anterior half of the meniscus (ML w-ant), and the maximum width of the posterior half of the meniscus (ML w-post). The ratio of enclosure was defined mathematically as the ratio of the AP depth to the distance between the horn attachments in the AP direction (Fig. 1b).

The cross section of the body of each meniscus was defined by five standard parameters in each of three regions. Each meniscus was divided into 10 sectors with equal arc length by transecting the outer edge of the meniscus at nine locations (Fig. 1a). An x-z reference frame was applied to each transection to acquire the five parameters used to describe the cross section (Fig. 1b). The x-axis was drawn parallel to the standardized transverse plane through the inner edge of the meniscus. The z-axis was drawn through the highest point on the meniscus perpendicular to the x-axis. Five cross-sectional parameters were used to describe the cross section: the maximum width of the meniscus (w), the maximum height of the meniscus (h), the bulge (b), a height ratio (h/h_o), and the slope (h_o/w_o). To obtain a representative description of the cross section while limiting the number

 DOI 10.1002/jor

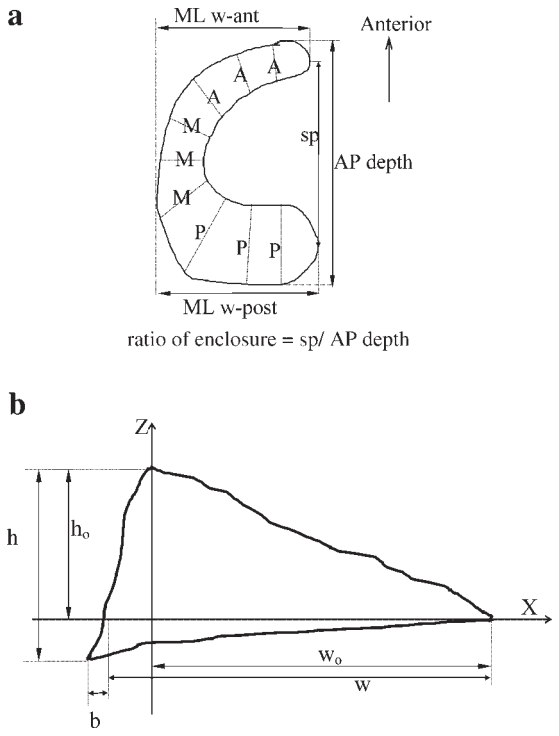

Figure 1. Schematic illustration of transverse and cross-sectional planes of the human meniscus. (a) Representation of the medial meniscus showing the four transverse parameters with the anterior, A, middle, M, and posterior, P regions. (b) Cross-sectional view of the meniscus showing the five measurements made to compute the five cross-sectional parameters (adapted from Haut and colleagues[14]).

of parameters to a manageable value, each of the five parameters was computed from the average of the three transections within the anterior, middle, and posterior regions.[14] Because they have been demonstrated previously to be important determinants of the contact pressure distribution on the tibial plateau,[11] the cross-sectional parameters of interest in this study were the height (h) and width (w) in each of the three regions.

Six transverse dimensions were measured from the MR images and included the width of the tibia (1_{MRI}), the depth of the medial (lateral) tibial plateau (2_{MRI}), the width of the femur (3_{MRI}), the depth of the medial (lateral) femur (4_{MRI}), the depth of the medial (lateral) meniscus (5_{MRI}), and the width of the medial (lateral) meniscus (6_{MRI}) (Fig. 2). These measurements were made using the scanner's system software to an accuracy of one pixel, approximately 500 μm.

Five cross-sectional (longitudinal) dimensions were measured from each of the anterior, middle, and posterior regions of each meniscus and were used to determine cross-sectional quantities using a previously described technique.[14] The three slices for measurement were chosen from the sagittal slice that most bisected the anterior region, the coronal slice that most bisected the middle region, and the sagittal slice that most bisected the posterior region. The five cross-sectional dimensions per region included the width (w_o) and maximum width (w), the height (h_o) and maximum height (h), and the bulge (b). In addition, the height ratio (h/h_o), width ratio (w/w_o), and slope (h_o/w_o) were also determined for each region. To provide a single quantity describing each of the eight cross-sectional quantities in each region, the average of each quantity was computed by averaging the respective values in each of the three regions. This resulted in a total of 32 MRI cross-sectional quantities (8 from three different regions and 8 averages).

Statistical analyses were performed using SAS software (Cary, NC) to develop the regression equations. A simple linear regression (significance at 0.05) was used to determine direct regression equations for each 3-DCDS parameter where the corresponding MRI dimension was used as the predictor variable. Because the ML w-ant, ML w-post, and ratio did not have corresponding MRI dimensions, no direct regression equations were computed for these parameters. To determine whether the predictive ability could be improved substantially over that of the direct regression equations and to determine regression equations for the three 3-DCDS parameters that had no corresponding MRI dimension, the best regression equations for each of the four transverse and six cross-sectional parameters were determined using a total of 38 predictor variables (24 cross-sectional quantities + 8 average cross-sectional quantities + 6 transverse quantities) measured from the MR images. The fit of the equations was assessed by calculating R^2 values. In those instances where the best regression equation improved the R^2 value over that of the direct regression equation by less than or equal to 0.1, the two equations were considered comparable in their predictive ability, and the direct regression equation was retained.

Diagnostic analyses were performed on the best equations to insure their propriety. Diagnostic tests included the creation of residual plots to check qualitatively the relation between the predictor and response variables, the equal variance assumption, and the normality of the error term. None of these diagnostics revealed that any remedial measures were necessary.

To evaluate quantitatively the potential effectiveness in using the best regression equations in an algorithm to select meniscal allografts, the standard deviation of the residuals (root mean squared error, RMSE) was determined for each equation. This standard deviation quantifies the random error associated with using the equations to predict the actual values of the meniscal parameters.

RESULTS

For the medial meniscus, the best regression equations predicted 8 of 10 (80%) medial meniscal parameters with R^2 values greater than 0.5 (Table 1). Transverse MRI quantities were either the best or comparable to the best predictor variables in three of these eight equations, and

cross-sectional MRI quantities were either the best or comparable to the best predictor variables in the remaining five equations. Nine MRI dimensions were required to determine these predictor variables and included the width (MRI w-ant, MRI w-mid, MRI w-post) and height (MRI h-ant, MRI h-mid, MRI h-post) in each of three regions plus the width of the tibia (1_{MRI}), the depth of the medial meniscus (5_{MRI}), and the width of the medial meniscus (6_{MRI}). Three of the seven

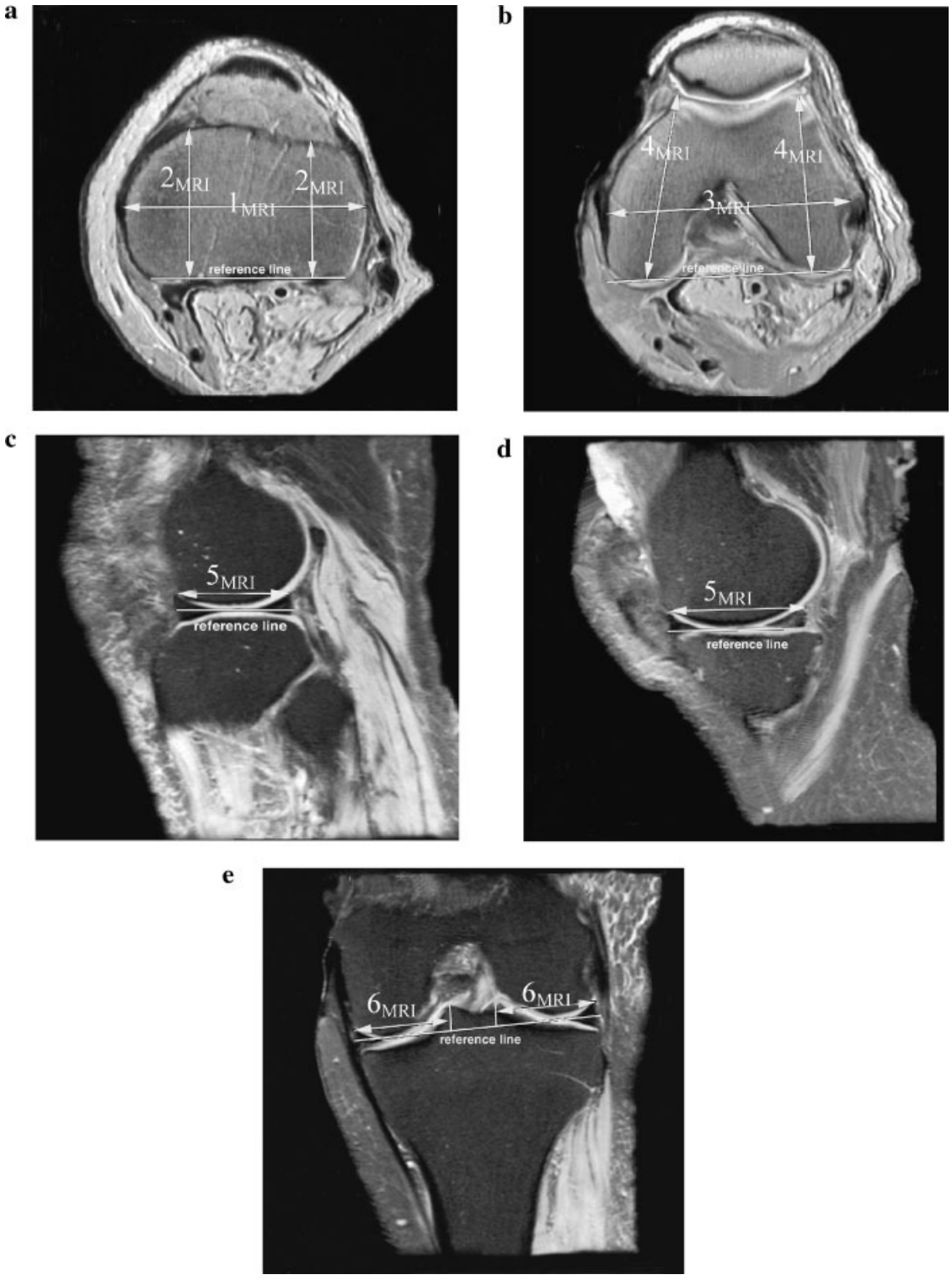

Figure 2.

 DOI 10.1002/jor

Table 1. Results of the Regression Analysis for the Medial Meniscus[a]

Medial Meniscal Parameter (Y)	Best Regression				
	Regression Equation	MRI Quantity (X)	R^2	RMSE	Tolerances[f]
h-ant	$Y = 3.932 + 0.295\ X$	MRI w-mid	0.338	1.29	+0.4/−0.3
h-mid	$Y = -3.000 + 1.631\ X$	MRI h-avg	0.731	1.00	+0.4/−0.3
h-post	$Y = 0.523 + 0.890\ X$	MRI h-post[c]	0.666	0.76	+0.4/−0.3
w-ant	$Y = 0.580 + 0.952\ X$	MRI w-ant[d]	0.667	1.80	+1.0/−0.9
w-mid	$Y = 5.100 + 0.749\ X$	MRI w-mid[d]	0.666	1.65	+1.0/−0.9
w-post	$Y = 0.468 + 1.267\ X$	MRI w-avg	0.746	1.44	+1.0/−0.9
AP depth	$Y = 9.071 + 0.719\ X$	5_{MRI}[d]	0.823	1.67	+1.6/−2.0
ML w-ant[b]	$Y = -37.169 + 0.832\ X$	1_{MRI}	0.670	2.83	+0.6/−0.9
ML w-post[b]	$Y = 2.011 + 0.765\ X$	6_{MRI}	0.681	1.61	+0.6/−0.9
Ratio[b]	$Y = 0.855 - 0.018\ X$	MRI w-mid	0.439	—[e]	N/A

[a]In the regression equations, Y is the predicted medial meniscal parameter and X is the MRI quantity. All dimensions are in mm.
[b]No matching MRI dimension.
[c]R^2 value of direct regression comparable to that of best regression.
[d]Same as direct regression.
[e]Value not provided because units of X and Y are not the same.
[f]Tolerances from Haut Donahue et al.[11]

direct regression equations were the same as the best regression equation. For one additional direct regression equation (h-post), the R^2 value of the direct regression equation was comparable (within 0.1) to that for the corresponding best regression equation.

For the lateral meniscus, the best regression equations predicted 10 of 10 (100%) lateral meniscal parameters with R^2 values greater than 0.5 (Table 2). Transverse MRI quantities were either the best or comparable to the best predictor variables in 5 of these 10 equations and cross-sectional MRI quantities were either the best or comparable to the best predictor variables in the remaining 5 equations. Nine MRI dimensions were required to determine these predictor variables

Figure 2. MRI images showing the transverse, sagittal and coronal views from which MRI measurements were made. (a) A reference line was drawn intersecting the most posterior edge of the tibial plateau on the transverse image closest to the joint line, the width of the tibia was measured parallel to the reference line (1_{MRI}), and the depths of the medial (2_{MRI}) and lateral (2_{MRI}) tibial plateaus were perpendicular to the reference line; (b) A reference line was drawn intersecting the most posterior edge of the femoral condyles on the transverse image with the largest femoral condyles, the width of the femur was measured parallel to the reference line (3_{MRI}), and the depths of the medial (4_{MRI}) and lateral (4_{MRI}) femur were measured as the distances from the anterior most point within each section of the femur and the reference line in the center of the posterior condyles. (c) The depth of the medial meniscus was measured from the sagittal image that best bisected the medial compartment. A reference line was drawn through the tibial plateau, and the depth of the medial meniscus was measured parallel to the reference line (5_{MRI}). (d) The depth of the lateral meniscus was measured from the sagittal image that best bisected the lateral compartment. A reference line was drawn through the tibial plateau , and the depth of the lateral meniscus was measured parallel to the reference line (5_{MRI}). (e) The widths of the medial and lateral menisci were measured parallel to the articular surface of the tibia on the coronal image that best displayed the tibial spines. A reference line was drawn through the tibia and two lines were drawn perpendicular to the reference line and through the lateral and medial meniscis. The width of the medial (6_{MRI}) and lateral (6_{MRI}) meniscis was measured from the outer edge of each meniscus to the medial and lateral spines, respectively. Imaging was performed with a 1.5-T magnet (Signa, General Electric, Milwaukee, WI) with a dedicated knee coil. Images obtained used a spin-echo, proton-density weighted technique with a repetition time = 2,300 ms and an echo time = 17 ms. Three-millimeter-thick slices with a 1-mm gap were acquired with two signal acquisitions: a 12×12-cm field of view and a 256×224 matrix. The resolution was 500 μm.

Table 2. Results of the Regression Analysis for the Lateral Meniscus[a]

Lateral Meniscal Parameter (Y)	Best Regression				
	Regression Equation	MRI Quantity (X)	R^2	RMSE	Tolerances[f]
h-ant	$Y = 1.750 + 0.664\ X$	MRI h-ant[c]	0.618	0.79	+1.4/−1.3
h-mid	$Y = 1.110 + 0.847\ X$	MRI h-mid[c]	0.581	1.03	+1.4/−1.3
h-post	$Y = -1.653 + 1.390\ X$	MRI h-post[d]	0.765	1.12	+1.4/−1.3
w-ant	$Y = 1.797 + 0.883\ X$	MRI w-ant[d]	0.568	1.56	+3.2/−1.7
w-mid	$Y = -1.004 + 0.284\ X$	2_{MRI}	0.582	1.27	+3.2/−1.7
w-post	$Y = 1.573 + 0.929\ X$	MRI w-post[c]	0.678	1.26	+3.2/−1.7
AP depth	$Y = -5.755 + 1.152\ X$	5_{MRI}[c]	0.504	3.76	+4.0/−2.0
ML w-ant[b]	$Y = -2.091 + 0.998\ X$	6_{MRI}	0.656	2.18	+3.2/−1.6
ML w-post[b]	$Y = -3.779 + 1.119\ X$	6_{MRI}	0.759	1.90	+3.2/−1.6
Ratio[b]	$Y = 0.783 - 0.003\ X$	3_{MRI}	0.620	—[e]	N/A

[a] In the regression equations, Y is the predicted lateral meniscal parameter and X is the MRI quantity. All dimensions are in mm.
[b] No matching MRI dimension.
[c] R^2 value of direct regression comparable to that of the best regression.
[d] Same as direct regression.
[e] Value not provide because units of X and Y are not the same.
[f] Tolerances from Haut Donahue et al.[11]

and included the height in each of three regions, the width in the anterior and posterior regions plus the depth of the lateral tibial plateau (2_{MRI}), width of the femur (3_{MRI}), depth of the lateral meniscus (5_{MRI}), and width of the lateral meniscus (6_{MRI}). Two of the seven direct regression equations were the same as the best regression equation. For four additional regression equations (h-ant, h-mid, w-post, and AP depth), the direct regression equation exhibited R^2 values comparable (within 0.1) to that for the best regression equation.

The regression equations predicted parameter values such that the errors from actual values were comparable for both medial and lateral menisci. The average RSME of the parameter values predicted by the regression equations were 1.56 mm and 1.65 mm for the medial and lateral menisci, respectively. For the medial meniscus, the lowest RMSE occurred for h-post and was 0.76 mm, while the highest RMSE occurred for ML w-ant and was 2.83 mm (Table 1). For the lateral meniscus, the RMSE ranged from 0.79 mm for h-ant to 3.76 mm for the AP depth (Table 2).

An algorithm, which incorporates the regression equations to select an allograft that best matches the size and shape of the damaged meniscus for a recipient, consists of the following steps:

Step 1) Determine transverse and cross-sectional parameters for an inventory of meniscal allografts using a tool such as the 3-DCDS.

Step 2) Take MR images of the recipient's uninjured knee.

Step 3) Measure nine dimensions for either the medial or lateral meniscus from the MR images and determine the predictor variables from these dimensions.

Step 4) Use these predictor variables in the regression equations in either Table 1 (medial meniscus) or Table 2 (lateral meniscus) to compute the values of the meniscal parameters that need to be matched.

Step 5) Screen all meniscal allografts in the inventory to identify candidate allografts such that the error between each parameter value of the allograft and the corresponding parameter value computed from the regression equations is less than previously determined tolerances[11] (Tables 1 and 2). Mathematically, the error for a particular parameter i denoted by err_i is determined as follows:

$$err_i = Ya_i - Yp_i \quad (1)$$

where Ya_i denotes the value of a meniscal parameter in the allograft inventory and Yp_i denotes the computed value of a meniscal parameter from the regression equations. The error must then satisfy:

$$|err_i| \leq |tol_i| \quad (2)$$

where tol_i is the corresponding tolerance for that parameter. Because the tolerances are bilateral and are not equal for positive and negative errors, the tolerance entered into Equation (2) should reflect the sign of err_i; if err_i is positive (negative), then the positive (negative) tol_i is used in Equation (2).

Step 6) Select the best allograft from the group of candidates identified in Step 5 by identifying the allograft that minimizes the sum of the weighted

 DOI 10.1002/jor

errors squared. Mathematically a weighting factor W_i is computed as:

$$W_i = RMSE_i/|tol_i| \quad (3)$$

This weighting factor reflects the wide variation in both the RMSE values and the tolerances (Tables 1 and 2). The best allograft is the one that minimizes the sum of weighted errors squared given by:

$$\min J = \sum_{i=1}^{9} (W_i err_i)^2. \quad (4)$$

Thus, a J-value is computed for each candidate allograft, and the allograft that provides the minimum J-value is the one selected. Note that the summation includes 9 of the 10 meniscal parameters because no tolerance has yet been determined for the ratio of enclosure.

DISCUSSION

Because both transverse and cross-sectional meniscal parameters are important determinants of the contact pressure distribution on the tibial plateau[11,12] and because no algorithm currently exists for selecting a meniscal allograft which matches the values of these parameters for a damaged meniscus, the primary objective of this study was to develop an algorithm for selecting meniscal allografts that matches both transverse and cross-sectional parameters. As a foundation for this algorithm, simple linear regression equations that predicted the medial and lateral meniscal parameters known to be determinants of the contact pressure distribution on the tibial plateau were developed.

In developing the regression equations, the meniscal parameters were limited primarily to those that have been demonstrated previously to be important determinants of the contact pressure.[11] The ratio of enclosure has not been demonstrated previously to be an important determinant of the contact pressure; nevertheless it was included because of evidence indicating the importance of this parameter. A previous study demonstrated that the placement of the posterior horn on the tibial plateau was an important determinant of the contact pressure.[17] Because varying the placement of the horn particularly in the AP direction effectively varies the ratio of enclosure, it can be inferred from these results that the ratio is also an important determinant of the contact pressure.

The random error of the regression equations as quantified by the RMSEs stemmed from two sources, which were any anatomical mismatch (i.e., side-to-side differences) between the injured and contralateral knees, and the limited resolution inherent in measuring tissue dimensions from MR images. The errors contributed by each of these sources have been determined previously but only for two transverse parameters, the AP depth and the width.[15] These errors ranged from 1.3 to 3.4 mm on average for measuring tissue dimensions from MR images and from 1.3 to 4.4 mm for side-to-side differences. In all cases, the errors for the medial meniscus were greater than the corresponding errors for the lateral meniscus.

Based on these results, it might be expected that the RMSEs of direct regression equations for these parameters would be greater for the medial than lateral meniscus. This expectation was not met by the results of the present study where the RMSEs were comparable for both medial and lateral menisci. Failure to meet this expectation may have been due to the different methods used to measure the tissue dimensions and obtain the MR images between the two studies. Regardless, because the errors from the two sources are comparable, it is likely that if the MRI resolution is improved, such as through the use a higher field strength MR system (e.g., 3 T), then the RMSEs of the regression equations would also likely improve.

To put the RMSE values into proper perspective requires additional information relating errors in predicted meniscal parameter values to changes in the contact pressure distribution on the tibial plateau.[14,15] For example, a previous study[11] determined the allowable errors or tolerances on meniscal parameter values to maintain the contact pressure distribution on the tibial plateau to within 10% of that of the normal knee. Our regression equations will predict values of meniscal parameters that fall within these tolerances 38% and 82% of the time for medial and lateral meniscal parameters, respectively. The disparity in these percentages can be attributed to smaller tolerances for medial than lateral meniscal parameters and to the comparable RMSE values for the medial and lateral menisci (Tables 1 and 2).

A relatively large RMSE does not translate into an inconsistent prediction of a particular meniscal parameter if the corresponding tolerance is also large. The largest RMSEs exceeded 2 mm for three parameters including ML w-ant for both the medial and lateral menisci and the AP depth for the lateral meniscus (Tables 1 and 2). However, for both the AP depth and ML w-ant for the lateral meniscus, the tolerances to maintain the contact pressure distribution on the tibial plateau to within 10% of that of the normal knee were also large, so that

predicted parameter values will fall within these tolerances 56% and 70% of the time for the AP depth and ML w-ant, respectively.

To implement the algorithm, tissue banks would need to determine the four transverse and six cross-sectional parameters for each allograft in the inventory using a tool such as the 3-DCDS. In using the 3-DCDS for this purpose, the procedures used in the present study would need to be adapted because allografts to be used for implantation in humans in vivo are harvested using bone blocks which span the anterior and posterior horns.[18] In the present study, however, the menisci were removed from the tibial plateau by resecting the anterior and posterior horns while leaving the bone intact.

Our procedure outlined in Step 6 to select the best allograft from the group of candidates that satisfy Equation (2) considers the two sources of error inherent to the selection process. One source is the error computed according to Equation (1), and the other source is the error inherent to the regression equations (RMSEs). To reflect the latter errors, a nondimensioned weighting factor for each parameter was introduced in Equation (3) owing to the wide variation in the RMSEs and tolerances between the parameters. For example, ML w-ant for the medial meniscus has a high weighting factor of 4.72 for the positive tolerance, in contrast to h-ant for the lateral meniscus that has a low weighting factor of 0.56 for the positive tolerance. A high weighting factor indicates a greater possibility for the regression equation to predict a parameter value that exceeds the tolerance by a greater amount than a low weighting factor. The quantitative rule for selecting the best allograft given by Equation (4) minimizes the sum of weighted errors squared so that large errors, which cause greater differences in the contact pressure distribution from normal than small errors,[11] are minimized with much stronger preference than small errors.

While both Steps 5 and 6 rely on tolerances that limit the difference in the contact pressure distribution to within 10% of that of the normal knee, no previous research known to the authors has determined what relative change in the contact pressure distribution accelerates the rate of cartilage wear. However, peak contact stresses on the lateral and medial articular surfaces of the tibia increase over 300% in the meniscectomized knee,[3,4,19,20] and contact areas decrease by 50%.[3,4,19,21] Thus, changes of only 10% could be assumed to reduce the rate of cartilage wear relative to that of the meniscectomized knee.

Not only is our algorithm useful in the short term for the selection of meniscal allografts, but also the algorithm will be useful in the long term for the selection of meniscal replacements other than allografts, including collagen scaffolds,[22] prosthetic menisci constructed from either Dacron,[23,24] Teflon[23] or porous polyurethane,[25] autologous fat pads,[26] small intestinal submucosa,[27] and autologous perichondral tissue.[28] Of these, only collagen scaffolds have been tested in humans to date with some promising results,[22] while the others are more preliminary with testing restricted to animal models. Any of these options or other replacement option(s) may likely emerge as viable tissue engineering options. Regardless of the material used in the replacement, it will still be advantageous to match the replacement to the size and shape of the original meniscus, in which case our algorithm should be useful.

While this study concentrated on improving the procedures of allograft selection by better matching the size and shape of a donor meniscus to that of a recipient, biomechanical variables other than size and shape should also be considered in the selection process. For example, the material properties of the meniscal tissue are also important determinants of the contact pressure distribution.[29,30] Accordingly, procedures should be developed for selecting allografts that are matched not only in size and shape, but also in material properties, particularly the circumferential tensile and the axial-radial compressive moduli.[29]

Other biomechanical factors may also be important determinants of the contact pressure distribution provided by an allograft. Two additional factors are placement of the allograft on the tibial plateau[17] and the method used to attach the allograft to surrounding tissues.[31,32] However, these two factors are differentiated from the size and shape and material properties because they are under the control of the surgeon and not the tissue bank.

In summary, we demonstrated that 8 of 10 medial and 10 of 10 lateral meniscal parameters, that are known to be important determinants of the contact pressure distribution on the tibial plateau, were predicted with R^2 values >0.5 by simple linear regression equations based on predictor variables determined from MRI scans. We also demonstrated that these predictor variables were determined from a total of nine dimensions measured from MRI scans. The regression equations were incorporated into an algorithm, which relies on proven technologies for input data. Accordingly, this algorithm can be implemented by a technician working in a

 DOI 10.1002/jor

tissue bank to select donor menisci that are matched in size and shape to the damaged meniscus in the recipient's knee. In using this algorithm, deviations in the predicted parameter values from the actual parameter values will be comparable for both menisci.

ACKNOWLEDGMENTS

The financial support of the Whitaker Foundation is gratefully acknowledged.

REFERENCES

1. Verdonk R. 2002. Meniscal transplantation. Acta Orthop Belg 68:118–127.
2. Ahmed AM, Burke DL. 1983. In-vitro measurement of static pressure distribution in synovial joints—part I: tibial surface of the knee. J Biomech Eng 105:216–225.
3. Baratz ME, Fu FH, Mengato R. 1986. Meniscal tears: the effect of meniscectomy and of repair on intraarticular contact areas and stress in the human knee. A preliminary report. Am J Sports Med 14:270–275.
4. Paletta GA Jr, Manning T, Snell E, et al. 1997. The effect of allograft meniscal replacement on intraarticular contact area and pressures in the human knee. A biomechanical study. Am J Sports Med 25:692–698.
5. Goble EM, Kohn D, Verdonk R, et al. 1999. Meniscal substitutes—human experience. Scand J Med Sci Sports 9:146–157.
6. Alhalki MM, Hull ML, Howell SM. 2000. Contact mechanics of the medial tibial plateau after implantation of a medial meniscal allograft. A human cadaveric study. Am J Sports Med 28:370–376.
7. Cameron JC, Saha S. 1997. Meniscal allograft transplantation for unicompartmental arthritis of the knee. Clin Orthop Rel Res 337:164–171.
8. Rath E, Richmond JC, Yassir W, et al. 2001. Meniscal allograft transplantation. Two-to-eight year results. Am J Sports Med 29:410–414.
9. van Arkel ER, de Boer HH. 2002. Survival analysis of human meniscal transplantations. J Bone Joint Surg [Br] 84:227–231.
10. Rodeo SA. 2001. Meniscal allografts—where do we stand? Am J Sports Med 29:246–261.
11. Haut Donahue TL, Hull ML, Rashid MM, et al. 2004. The sensitivity of tibiofemoral contact pressure to the size and shape of the lateral and medial menisci. J Orthop Res 22:807–814.
12. Huang A, Hull ML, Howell SM, et al. 2002. Identification of cross-sectional parameters of lateral meniscal allografts that predict tibial contact pressure in human cadaveric knees. J Biomech Eng 124:481–489.
13. L'Insalata J, Klatt B, Caravaggio H, et al. 1996. Accuracy and reliability of office techniques for meniscal allograft sizing. Marietta, GA: Cryolife Corp.
14. Haut TL, Hull ML, Howell SM. 2000. Use of roentgenography and magnetic resonance imaging to predict meniscal geometry determined with a three-dimensional coordinate digitizing system. J Orthop Res 18:228–237.
15. Shaffer B, Kennedy S, Klimkiewicz J, et al. 2000. Preoperative sizing of meniscal allografts in meniscus transplantation. Am J Sports Med 28:524–533.
16. Haut TL, Hull ML, Howell SM. 1998. A high-accuracy three-dimensional coordinate digitizing system for reconstructing the geometry of diarthrodial joints. J Biomech 31: 571–577.
17. Sekaran SV, Hull ML, Howell SM. 2002. Nonanatomic location of the posterior horn of a medial meniscal autograft implanted in a cadaveric knee adversely affects the pressure distribution on the tibial plateau. Am J Sports Med 30:74–82.
18. Felix NA, Paulos LE. 2003. Current status of meniscal transplantation. Knee 10:13–17.
19. Kurosawa H, Fukubayashi T, Nakajima H. 1980. Load-bearing mode of the knee joint: physical behavior of the knee joint with or without menisci. Clin Orthop 149:283–290.
20. Seedhom BB, Hargreaves DJ. 1979. Transmission of the load in the knee joint with special reference to the role of the menisci. Eng Med 8:220–228.
21. Fukubayashi T, Kurosawa H. 1980. The contact area and pressure distribution pattern of the knee. A study of normal and osteoarthrotic knee joints. Acta Orthop Scand 51:871–879.
22. Stone KR, Steadman JR, Rodkey WG, et al. 1997. Regeneration of meniscal cartilage with use of a collagen scaffold. Analysis of preliminary data. J Bone Joint Surg [Am] 79:1770–1777.
23. Messner K. 1994. Meniscal substitution with a Teflon-periosteal composite graft: a rabbit experiment. Biomaterials 15:223–230.
24. Sommerlath K, Gillquist J. 1993. The effects of an artificial meniscus substitute in a knee joint with a resected anterior cruciate ligament. An experimental study in rabbits. Clin Orthop Rel Res 289:276–284.
25. Klompmaker J, Veth RP, Jansen HW, et al. 1996. Meniscal replacement using a porous polymer prosthesis: a preliminary study in the dog. Biomaterials 17:1169–1175.
26. Kohn D, Rudert M, Wirth CJ, et al. 1997. Medial meniscus replacement by a fat pad autograft. An experimental study in sheep. Intl Orthop 21:232–238.
27. Cook JL, Tomlinson JL, Kreeger JM, et al. 1999. Induction of meniscal regeneration in dogs using a novel biomaterial. Am J Sports Med 27:658–665.
28. Bruns J, Kahrs J, Kampen J, et al. 1998. Autologous perichondral tissue for meniscal replacement. J Bone Joint Surg [Br] 80:918–923.
29. Haut Donahue TL, Hull ML, Rashid MM, et al. 2003. How the stiffness of meniscal attachments and meniscal material properties affect tibio-femoral contact pressure computed using a validated finite element model of the human knee joint. J Biomech 36:19–34.
30. Spilker RL, Donzelli PS. 1992. A biphasic finite element model of the meniscus for stress-strain analysis. In: Mow VC, Arnoczky SP, Jackson DW, editors. Knee meniscus: basic and clinical foundations. New York: Raven Press p 91–106.
31. Alhalki MM, Howell SM, Hull ML. 1999. How three methods for fixing a medial meniscal autograft affect tibial contact mechanics. Am J Sports Med 27:320–328.
32. Chen MI, Branch TP, Hutton WC. 1996. Is it important to secure the horns during lateral meniscal transplantation? A cadaveric study. Arthroscopy 12:174–181.